RESEARCH PAPER

PCCP
www.rsc.org/pccp

Clustering of water molecules in aqueous solutions: Effect of water–solute interaction†

Ivan Brovchenko,[a] Alfons Geiger[a] and Alla Oleinikova[b]

[a] *Physical Chemistry, University of Dortmund, Otto-Hahn-Str. 6, 44221, Dortmund, Germany. E-mail: brov@heineken.chemie.uni-dortmund.de, alfons.geiger@udo.edu*
[b] *Physical Chemistry, Ruhr-University Bochum, Universitätsstr. 150, 44780, Bochum, Germany. E-mail: alla.oleinikova@ruhr-uni-bochum.de*

Received 11th November 2003, Accepted 23rd December 2003
First published as an Advance Article on the web 23rd January 2004

Clustering of water molecules in partially miscible aqueous solutions (with immiscibility gap) was studied by Monte Carlo (MC) simulations. Liquid–liquid coexistence curves were determined by MC simulations in the Gibbs ensemble. Water cluster size distributions were studied in the organic-rich one-phase region. At the coexistence curve we observe the broadest distribution of cluster sizes in agreement with the Fisher droplet model. There are no percolating water clusters in aqueous mixtures of solutions of hydrophobic particles in the studied concentration range. In contrast, in an aqueous solution of hydrophilic solutes crossing the coexistence curve approximately coincides with the 3D percolation threshold of water. An infinite water cluster (percolating cluster or droplet of the second phase) appears in an aqueous solution, when the average number of water–water H-bonds per molecule exceeds *ca.* 1.6.

1 Introduction

The arrangement of molecules on a mesoscopic level essentially effects all properties of fluid mixtures. Structural microheterogeneities of aqueous solutions were detected in numerous experimental studies even in aqueous solutions of simple solutes. It is convenient to analyse such microheterogeneities using clustering concepts, grouping all molecules into clusters, based on some criteria of connectivity between pairs of molecules. The main goal of the clustering analysis is to obtain cluster size distributions, *i.e.* the occurrence frequency of cluster sizes. These distributions vary with concentration and temperature, in particular, when approaching a possible immiscibility gap.

Experimental studies allow to estimate the population of various clusters in mixtures only if the effect of the cluster size distribution on some measured properties is known. This is a rarely the case, especially for concentrated solutions (see, for example, refs. 1 and 2). Some information concerning cluster populations could be obtained from mass spectra of aqueous solutions.[3] However, the relation between such spectra and the cluster size distributions in the liquid is still unclear. Note also that X-ray scattering measurements of aqueous solutions in a wide concentration range were interpreted as indication for the formation of an infinite water network, *i.e.* for the appearance of a percolating cluster.[4]

There are two qualitatively distinct major theoretical approaches, which predict the size distribution of molecular clusters. The percolation theory describes the population of clusters in a system when it approaches the percolation threshold, which is indicated by the appearance of an infinite cluster. The percolation threshold should coincide with the thermodynamic critical point of Ising magnets and pure fluids, when the proper criterion for a physical cluster is used.[5] Indeed, this was observed for a Lennard-Jonnes fluid, when two molecules are considered as connected, if the magnitude of the (negative) potential energy exceeds their relative kinetic energy[6,7] (see ref. 8 for a recent review). A line of percolation thresholds was found above the critical temperature, while the location (or even existence) of a percolation transition in the subcritical region is unclear.

The Fisher droplet model[9] describes the distribution of clusters below the critical temperature both apart and at the coexistence curve. Simulations of 2D Ising systems[10] and recent experimental studies of the multifragmentation of excited nuclear matter[11] strongly support this model. However, its applicability to 3D Ising system is questionable[12] and is still an area of debates.[13,14]

Clustering, including the formation of an infinite network, could be studied by integral equation theory[15,16] or by computer simulations. In any study of clustering the choice of the criteria of the connectivity between molecules has a crucial effect on the results (see refs. 7 and 8 and references therein). Such a criterion is physically obvious for water molecules (compared to, for example, Lennard-Jonnes particles), as it is based on the existence of highly-directional and short-ranged hydrogen bonds. That is why clustering in liquid water, including the appearance of percolation clusters, was studied in detail.[17,18] Recently, water clustering was studied in tetrahydrofuran (THF) + water (W) mixtures in a wide concentration range including the proximity of the rather narrow immiscibility region.[19] A two-step percolation of water was observed in these mixtures. When the water mass fraction achieves $C = 0.19$ a 2D percolation network occurs in the solution, while the 3D water percolation threshold (at $C = 0.30$) practically coincides with the organic branch of the coexistence curve. It was found that the two-phase region approximately corresponds to the concentration range where both components form an infinite 3D percolation network.[19] In solutions with a wider immiscibility gap demixing occurs at lower water concentrations, which may be below the percolation threshold for water. The behaviour of water clusters in such systems is not clear.

In the present paper we study the evolution of water clustering in aqueous solutions when approaching and crossing the

† Presented at the 81st International Bunsen Discussion Meeting on "Interfacial Water in Chemistry and Biology", Velen, Germany, September 19–23, 2003.

DOI: 10.1039/b314474g

organic-rich branch of a liquid–liquid coexistence curve. Two model systems are compared: aqueous solutions of hydrophobic and of hydrophilic solutes, which are immiscible in wider and narrower concentration ranges, respectively. The possibility to use the analysis of water clustering in computer simulations for the location of the immiscibility region are discussed.

2 Simulation of the liquid–liquid coexistence in the Gibbs ensemble

The location of a possible immiscibility region is a necessary prerequisite condition to study any property of a model mixture, especially molecular clustering. The only simulated liquid–liquid coexistence curve of an aqueous solution was reported for a THF + W mixture,[20] where a five-site model for THF[21] and the TIP4P model for water[22] were used. For this mixture, multiplying the Coulombic cross-interaction between the THF and the water molecules by a factor $f = 1.2$ produced an immiscibility region close to the experimentally observed one (its maximal extension is from $X = 0.60$ to $X = 0.91$,[23] where X is the mole fraction of water). Without scaling the Coulombic cross-interaction ($f = 1.0$), the immiscibility gap is much broader[20] (see also Fig. 1). So, by varying the f factor we have the possibility to change the hydrophobicity (hydrophilicity) of the model solute in some range.

We consider two kinds of model THF solutes, which we call henceforth "hydrophobic THF" ($f = 1.0$) and "hydrophilic THF" ($f = 1.2$). If the lower value of f is used, the system size in the simulations had to be increased significantly due to the lower value of X at the organic-rich branch of the coexistence curve. At values of f higher than 1.2 the application of the Gibbs ensemble MC method becomes less reliable due to the strong interaction between THF and water molecules.

The liquid–liquid coexistence curve of the hydrophobic THF + W mixture was evaluated in the NPT Gibbs ensemble[24] at $P = 1$ bar. All parameters of the simulations (apart from the f factor) were the same as in the previous studies of the coexistence curve of the hydrophilic THF + W mixture. In particular, a cut-off for the intermolecular interactions was put equal to 8 A with long-range corrections for Lennard-Jonnes interaction only. The sizes of the simulation boxes varied from *ca.* 23–32 Å, and the total number of molecules in the two boxes was about 800 (see ref. 20 for other details of the simulations). The obtained liquid–liquid coexistence curve of the hydrophobic THF + W mixture is presented in Fig. 1 (the results for the hydrophilic THF + W mixture are also shown for comparison). The distortion of the coexistence curve at $T > 400$ K is most likely due to the simulations at constant pressure ($P = 1$ bar), and not at the saturated vapour pressure. At $T = 450$ K both coexisting phases are still liquids, whereas at $T = 475$ K they evaporate.

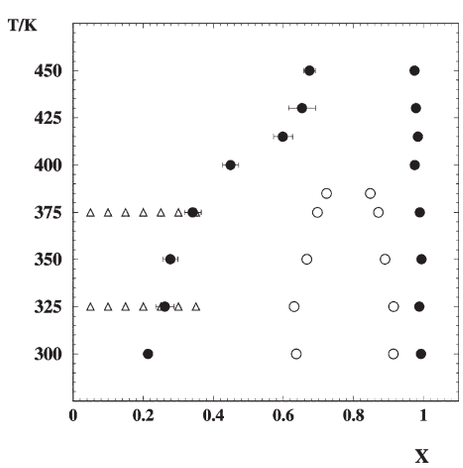

Fig. 1 Liquid–liquid coexistence curves of aqueous solutions of the hydrophobic THF (solid circles) and hydrophilic THF (open circles), see text. Triangles indicate the systems used for the analysis of water clustering in the hydrophobic THF. X is the mole fraction of water.

3 Analysis of water clustering

Analysis of the water clustering in the hydrophobic THF + W mixture was done for different compositions X in the organic-rich one-phase region at $T = 325$ K and $T = 375$ K. The studied systems are indicated in Fig. 1 by triangles. The organic-rich branch of the liquid–liquid coexistence curve of hydrophobic THF + W mixture is located at lower water contents, compared to the hydrophilic THF. Therefore, essentially larger system sizes were used for the analysis of water clustering in the former case (the size of the simulation box was 63.5 ± 0.3 Å for the hydrophobic THF and 26.5 ± 0.5 Å for the hydrophilic THF[19]). To estimate the effect of the system size on the cluster size distribution, the hydrophilic THF + W W mixture at $X = 0.30$ was additionally simulated in the large box. The total number of molecules in the simulation box varied from 1800 to 2300, whereas the number of water molecules varied from 90 to 800, depending on X. For each composition and temperature two different initial configurations were prepared by a random distribution of the molecules in the simulation box. After equilibration (5×10^4 MC steps per molecule), a total of about 1.5×10^5 MC steps per molecule in the NPT ($P = 1$ bar) ensemble were done for each system, and every 1000th configuration was used for the analysis of water clustering. The obtained equilibrium densities of the hydrophobic THF + W mixture are shown in Fig. 2 for all studied concentrations together with the densities of the hydrophilic THF + W mixture.[19]

Two water molecules are considered to belong to the same cluster if they are connected by a continuous H-bond network.

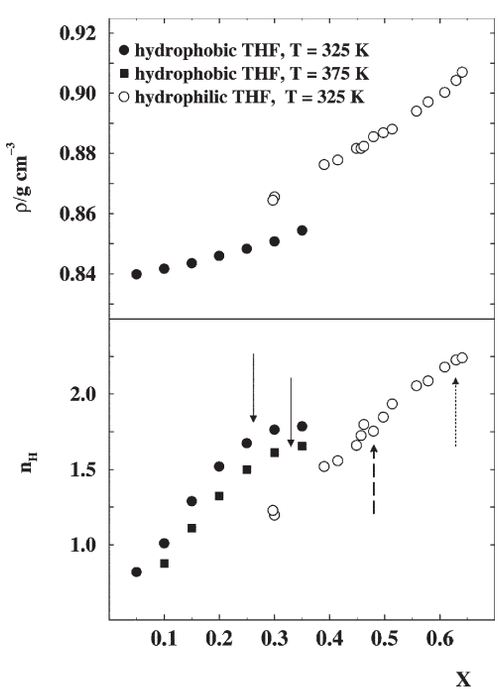

Fig. 2 Density, ρ, of aqueous solutions and average number n_H of water–water hydrogen bonds per molecule as a funcion of the water mole fraction X. The location of the organic-rich branches of the coexistence curves are shown by solid and dotted arrows for the aqueous solution of hydrophobic THF and hydrophilic THF, respectively. The dashed arrow indicates the 2D percolation threshold in the solution with hydrophilic THF.

A combined energy-distance H-bond criterion was used[19] ($V_{HB} \leq -2.6$ kcal mol, $r_{O\text{–}O,\ HB} \leq 3.5$ Å). The cluster size distribution $n_S(S)$, which is the probability to find clusters of size S (normalized by the total number of clusters in the considered configuration) was obtained for each concentration X. Besides, each configuration was inspected for the presence of an infinite (spanning) percolating cluster. See ref. 19 for more details of the analysis of water clustering.

4 Results

In all considered hydrophobic THF + W mixtures the existence of a percolating water cluster was never observed. The cluster size distributions of the water molecules in the studied hydrophobic THF + W mixtures are shown in Fig. 3 and Fig. 4 at $T = 325$ K and $T = 375$ K, respectively. With increasing water concentration X the distribution n_S extends towards larger cluster sizes S. The widest distribution of n_S is observed close to the organic-rich branch of the coexistence curve ($X_{CC} = 0.26$ at $T = 325$ K and $X_{CC} = 0.33$ at $T = 375$ K). Penetration into the two-phase region ($X = 0.30$, $X = 0.35$, Fig. 3 and $X = 0.35$, Fig. 4) causes a reverse trend, *i.e.* the distribution of n_S shrinks due to the dissappearance of the largest clusters.

Similar trends are observed in the size distributions n_S of water clusters in hydrophilic THF + W mixtures up to $X = 0.50$ (Fig. 5). At higher water concentrations the behaviour of n_S changes drastically due to the presence of the percolating water cluster. This quazi-infinite cluster appears as huge hump at high S and produces a strong decrease of the population of all finite clusters. The formation of a percolating cluster is illustrated in Fig. 6, where the fraction S^*n_S of water molecules in clusters of size S is shown for several mixtures (the percolation threshold is located at $X = 0.52$[19]).

Water clustering is essentially different when the hydrophobic THF + W mixture and the hydrophilic THF + W mixture are compared at the same concentration. The size distribution n_S extends to larger sizes S and the population of small clusters is lower in the case of hydrophobic THF (Fig. 7). For example, the fraction of water molecules which exist as monomers (not bound to another water molecule) in the hydrophilic THF + W mixture is about two times higher than in the case of hydrophobic THF (see Fig. 8). This difference disappears at $S \approx 8$ to 10, and the population of clusters with $S > 10$ is higher in the case of hydrophobic THF. The same trend appears in the distribution of water–water H-bonds per molecule (Fig. 9) and holds in the whole concentration interval which has been studied (Fig. 2).

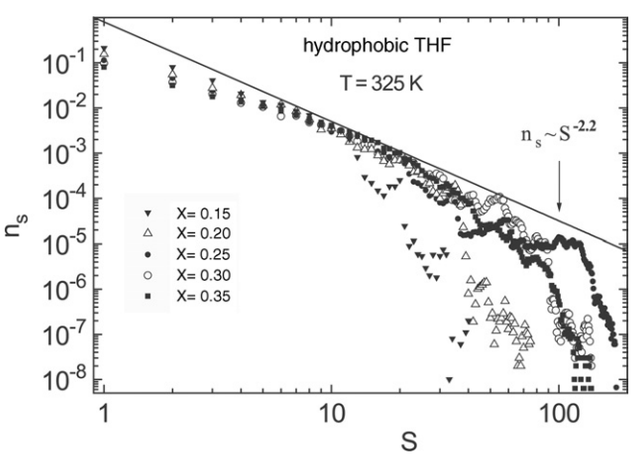

Fig. 3 Size distribution of water clusters in aqueous solutions of the hydrophobic THF at $T = 325$ K.

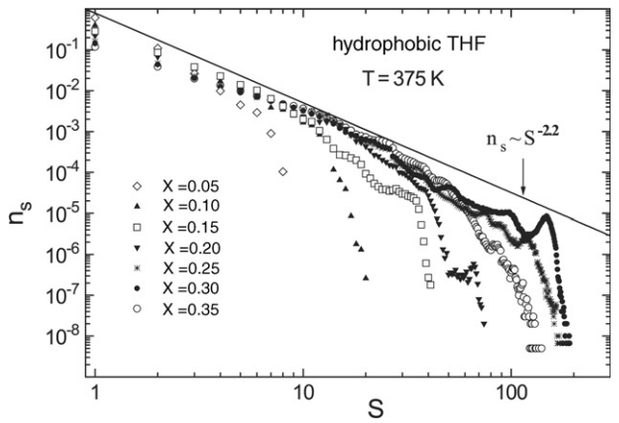

Fig. 4 Size distribution of water clusters in aqueous solutions of the hydrophobic THF at $T = 375$ K.

Note also that the population of the small clusters continuously decreases with increasing water concentration X in both studied systems (Figs. 3–5). This effect is clearly seen up to $S \approx 3$ to 4 at $T = 375$ K (Fig. 4) and extends up to $S \approx 7$ to 10 at $T = 325$ K (Figs. 3 and 5). In the case of the hydrophilic THF this trend disappears when approaching the coexistence curve with the formation of the 3D percolation water cluster (Fig. 5).

The system size has no significant influence on the distribution n_S, some noticeable effects occur at large clusters only (compare line and squares in Fig. 7).

5 Discussion

The changes of the cluster size distribution n_S which are observed when approaching the coexistence curve of the hydrophobic THF + W mixture (Figs. 3 and 4), agree qualitatively with the Fisher droplet model,[9] which predicts the following behaviour of n_S in the subcritical region:

$$n_S \sim S^{-\tau} \exp(S\Delta\mu/kT) \exp(-AS^{\sigma}/kT), \qquad (1)$$

where $\tau = 2.2$ is a universal exponent, $\Delta\mu = \mu - \mu_{cc}$ is the deviation of the chemical potential, μ, from its value μ_{cc} at the coexistence curve. σ is an exponent, which depends on the droplet shape and ranges from 2/3 (spherical droplet) to 1. A is related to the surface energy density of a droplet. The second exponential term, related to the surface tension, provides a relatively slow decay of n_S with increasing S (due to $\sigma < 1$) and does not change, when crossing the coexistence

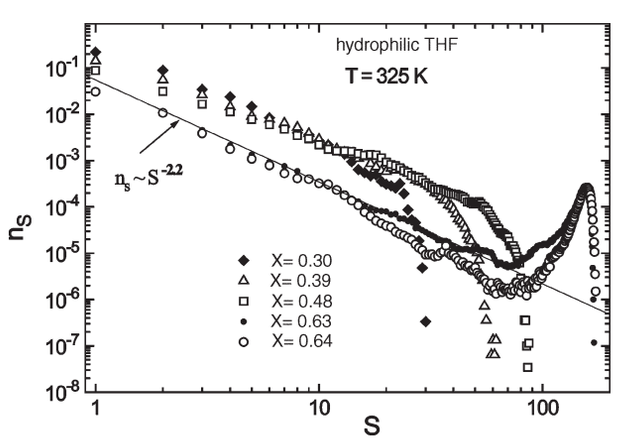

Fig. 5 Size distribution of water clusters in aqueous solutions of the hydrophilic THF at $T = 325$ K.

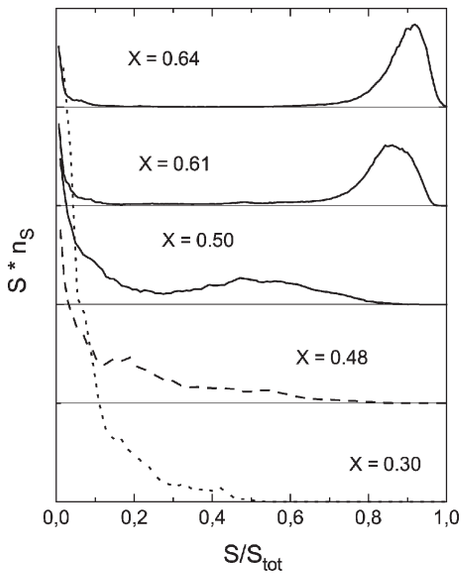

Fig. 6 Fraction S^*n_S of water molecules in clusters of size S in aqueous solutions of the hydrophilic THF as a function of cluster size (normalized by the total number of water molecules S_{tot}). Percolating clusters appear as a maximum of S^*n_S, which is broadest at the percolation threshold ($X = 0.53$). With increasing X this maximum becomes sharper and shifts towards higher values S/S_{tot}.

curve. The first exponential term provides a rapid decay of n_S far from the coexistence curve due to a large negative value of $\Delta\mu$. At the coexistence curve $\Delta\mu = 0$ and the slowest decay of n_S with S is expected. Crossing the coexistence curve provides $\Delta\mu > 0$ and should results in a strong increase of n_S at high S. Depending on their size, these large clusters may form a "nucleus" of the second phase or become unstable and desintegrated into smaller clusters during the separation of the system into two phases.

For infinite systems, one may expect in the whole two-phase region contributions to n_S from both coexisting phases and eqn. (1) is no more valid. In finite systems, however, the formation of a second phase occurs not exactly at the coexistence curve, but inside the two-phase region.[25–28] The behaviour of n_S in the corresponding concentration interval (inside the two-phase region, but in the absence of the second phase) is not clear.

Strictly speaking, our definition of clusters is correct for the percolation analysis, but not for droplet models. Application

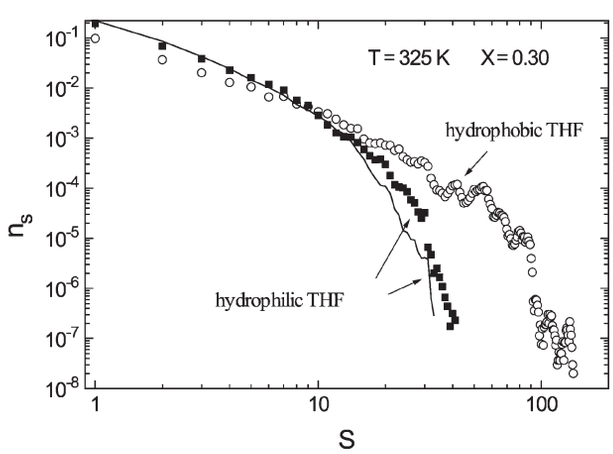

Fig. 7 Size distribution of water clusters in aqueous solutions of hydrophobic THF and hydrophilic THF. Systems of equal size were used (symbols). The line shows the distribution in a system, which contains 12 times less molecules.

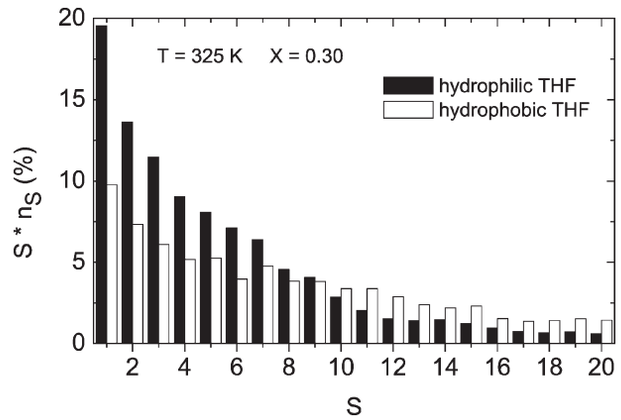

Fig. 8 Fraction S^*n_S of water molecules in clusters of size S.

of the Fisher droplet model to liquid–liquid phase transitions requires the consideration of droplets of "opposite" phase (water-rich phase in our case), and not pure water droplets.[29] In the studied THF + W mixtures we may in good approximation consider water clusters as clusters of the second, "opposite" phase, because its concentration is rather close to pure water ($X = 0.91$ and $X = 0.98$ in the case of hydrophilic and hydrophobic THF, respectively).

In the hydrophobic THF + W mixtures the decay of n_S becomes slower with increasing water concentration, when approaching the coexistence curve (Figs. 3 and 4), and the broadest n_S distribution is observed close to the coexistence curve in accordance with the Fisher droplet model.[9] The penetration into the two-phase region causes pronounced changes of n_S: it decays apparently more rapidly with increasing S due to the disintegration of the large clusters. The crossing of the coexistence curve may be detected also by calculating the mean cluster size $S_{mean} = \sum S^2 n_S / \sum S n_S$, and by locating the position of its maximum in the absence of the second phase in the simulation box (Fig. 10). At some level of penetration into the two-phase region the formation of "nuclei" of the second phase will presumably result in the appearance of a sharp peak at large S, separated from the main distribution n_S. However, the appearance of "macroscopic" clusters in the simulation box is not an indication of the crossing of the coexistence curve in finite systems.[25–28]

In the case of the hydrophilic THF + W mixture the behaviour of n_S is consistent with the Fisher droplet model up to the water concentration $X = 0.50$ (see Fig. 5). At higher water content the distribution n_S drastically changes due to the appearance of the infinite percolation clusters: also still in the one-phase region, percolation clusters form a pronounced

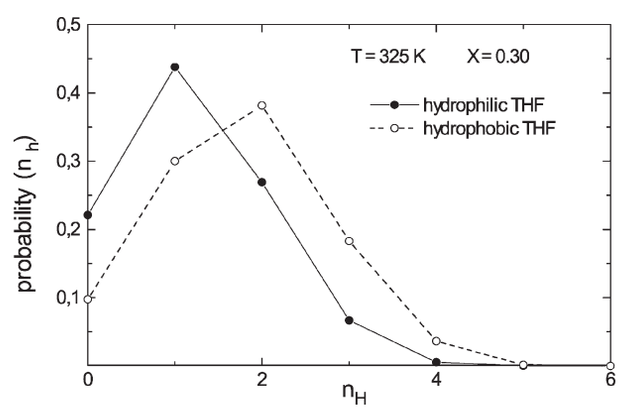

Fig. 9 Distribution of water molecules with n_H hydrogen bonds to the water molecules in solutions of hydrophobic THF and hydrophilic THF.

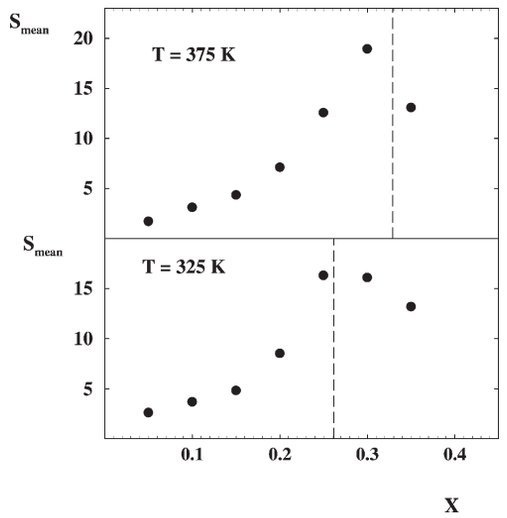

Fig. 10 Mean cluster size S_{mean} as a function of the water concentration X in hydrophobic THF + W mixtures. The location of the coexistence curve is indicated by a dashed line.

hump in the distribution n_S at large S; the population of all finite clusters drops sharply when approaching the coexistence curve and formation of the 3D percolation cluster occurs. The mean cluster size S_{mean}, which does not include the largest cluster, passes through a maximum in the one-phase region close to the coexistence curve.[19] Similar to the hydrophobic THF + W mixture (Figs. 3 and 4), penetration into the two-phase region of the hydrophilic THF + W mixture (Fig. 5) causes a drop of the occurrence probability of large clusters (excluding percolating clusters).

It is interesting to note that the average number of water–water H-bonds per molecule achieves $n_{\mathrm{H}} \approx 1.60$ to 1.75 both at the organic-rich branch of the coexistence curve of the hydrophobic THF + W mixture and at the percolation threshold of the hydrophilic THF + W mixture (Fig. 2). These values are close to the value $n_H = 1.53 \pm 0.05$ at the bond percolation threshold for pure liquid water, obtained when varying the H-bond definition,[18] and $n_{\mathrm{H}} = 1.60$, obtained near the water liquid–vapour critical point.[30] Above this value ($n_{\mathrm{H}} \approx 1.60$), an infinite water cluster (droplet of second phase or percolating cluster) appears in aqueous solution and in pure water.

The Fisher droplet model[9] is valid for large cluster sizes, when the potential energy per molecule does not depend on S. Indeed, we observed essential negative deviations of n_{S} for small clusters with $S < 10$ at $T = 325$ K in both hydrophobic (Fig. 3) and hydrophilic THF + W mixtures (Fig. 4 of ref. 19). Note that in the Ising model this effect is noticeable for $S < 8$ in 2D systems[10] and for $S < 11$ in 3D systems.[12]

The change of the clustering of molecules upon penetration into the two-phase region could be used for the location of the coexistence curve. Recently, the appearance of "macroscopic" clusters (a hump at the cluster size distribution at large S) was proposed as an indication of the crossing of the coexistence curve.[6] However, our results as well as the results of refs. 25–28 evidence that this is not the case in finite systems (see above). In a one-phase region the appearance of "macroscopic" clusters may be due to an approach to the percolation threshold in a finite system.[19] Therefore, we propose another method to locate an immiscibility region in any aqueous solution by a cluster analysis in computer simulations. It is based on the determination of cluster size distributions with increasing water concentration and an additional check for the presence of a percolating cluster. The maximum value of the mean cluster size S_{mean} (excluding the percolating cluster, if it exists) will indicate the position of the organic-rich branch of the coexistence curve. Note that the water-rich branch of the coexistence curve may be located in a similar way by using an appropriate criterion for the connectivity of the solute molecules.[6–8] The proposed scheme allows one to avoid simulations with two coexisting phases in one simulation box (and so, with an explicit interface). Alternatively, MC or molecular dynamics simulations in an NPT- or NVT-ensemble could be used, allowing one to estimate the location of the liquid–liquid coexistence curve of an aqueous solution, when all other available methods (simulations in the Gibbs ensemble in particular) fail.

Our results identify three possible kinds of aqueous solutions with respect to the formation of an infinite H-bonded water network. In mixtures of the first kind with hydrophobic solutes (like the hydrophobic THF + W mixture studied in the present paper) the network appears only at water concentrations, exceeding the concentration of the water-rich branch of the coexistence curve. For the mixture of the second kind with more hydrophilic solutes (like in the hydrophilic THF + W mixture studied in ref. 19) the immiscibility region is narrower and the water network exists both in the water-rich and organic-rich phases. As discussed in ref. 19 an infinite water network appears as a 2D percolating cluster at some critical water concentration and becomes a 3D percolating cluster approximately at the organic-rich branch of the coexistence curve. The formation of a 2D water network may be considered as a quasi-two-dimensional "condensation" of water on the "surface" of the solute molecules or of solute clusters.[31] Its 2D character is indicated by the fractal dimension[19] and also by the appearance of a specific hump in the pair correlation function at a water oxygen–oxygen distance of $r = 5.5$ Å. This corresponds to twice the distance of the first maximum $g_{\mathrm{O-O}}(r)$ (Fig. 11). The same correlation appears in the water layer at a hydrophilic smooth surface.[32] The water weight fraction $C = 0.19$ [19] at the 2D percolation threshold is comparable to the reported values $C = 0.10$ to 0.20 for the 2D percolation threshold of water in hydrated biological molecules.[33–39] This threshold coincides with the onset of water-induced functionality of biological molecules.

Further strengthening of the water–solute interaction shifts the water percolation threshold towards higher concentrations

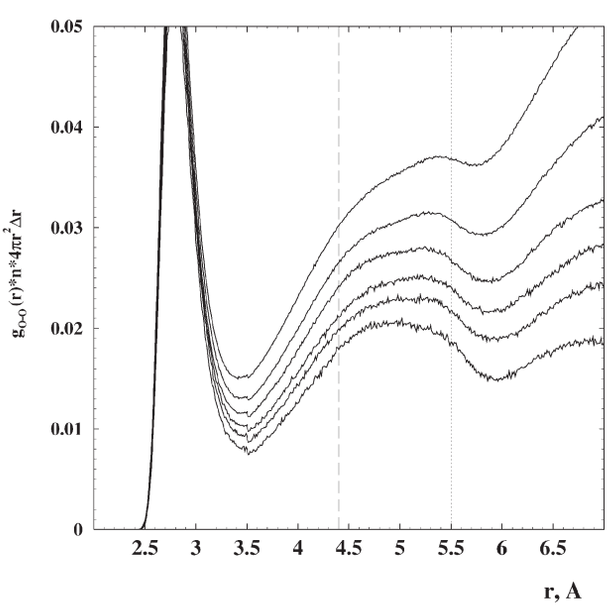

Fig. 11 Evolution of the radial distribution function $g_{\mathrm{O-O}}(r)^* n^* 4\pi r^2 \Delta r$ within the largest water cluster in hydrophilic THF + W mixture with increasing water concentration X from 0.30 (bottom curve) to 0.63 (top curve). n is the number density of water. Dashed and dotted lines indicate the position of the tetrahedrally bound second neighbours and twice the distance of the first maximum of bulk water, respectively.

and makes the solution completely miscible (mixture of the third kind). We may expect that in such solutions there is a concentration interval where both components are below their respective 3D percolation thresholds.[19] This assumption agrees with experimental studies[4] and should be tested by computer simulations.

Acknowledgements

We would like to thank M. E. Fisher and M. Holovko for stimulating discussions. Financial support from DFG Forschergruppe 436 is gratefully acknowledged.

References

1 V. A. Durov, *J. Mol. Liq.*, 2003, **103–104**, 41.
2 T. Koddermann, F. Schulte, M. Huelsekopf and R. Ludwig, *Angew. Chem.*, 2003, **115**, 5052.
3 D. A. Shin, J. W. Wijnen, B. F. N. Engberts Jan and A. Wakisaka, *J. Phys. Chem. B*, 2002, **106**, 6014.
4 T. Takamuku, A. Nakamizo, M. Tabata, K. Yoshida, T. Yamaguchi and T. Otomo, *J. Mol. Liq.*, 2003, **103–104**, 143.
5 A. Coniglio and W. Klein, *J. Phys. A*, 1980, **13**, 2775.
6 X. Campi, H. Krivine and N. Sator, *Nucl. Phys. A*, 2001, **681**, 458c; *Physica A*, 2001, 296, 24.
7 L. A. Pugnaloni, I. F. Marquez and F. Vericat, *Physica A*, 2003, **321**, 398; L. A. Pugnaloni and F. Vericat, *J. Chem. Phys.*, 2002, **116**, 1097.
8 N. Sator, *Phys. Rep.*, 2003, **376**, 1.
9 M. E. Fisher, *Physics*, 1967, **3**, 255.
10 E. Stoll, K. Binder and T. Schneider, *Phys. Rev. B*, 1972, **6**, 2777.
11 J. B. Elliott, L. G. Moretto, L. Phair, G. J. Wozniak, L. Beaulieu, H. Breuer, R. G. Korteling, K. Kwiatkowski, T. Lefort, L. Pienkowski, A. Ruangma, V. E. Viola and S. J. Yennello, *Phys. Rev. Lett.*, 2002, **88**, 42 701.
12 H. Muller-Krumbhaar and E. P. Stoll, *J. Chem. Phys.*, 1976, **65**, 4294.
13 F. Gulminelli, Ph. Chomaz, M. Bruno and M. D'Agostino, *Phys. Rev. C*, 2002, **65**, 51 601.
14 C. M. Mader, A. Chappars, J. B. Elliott, L. G. Moretto, L. Phair and G. J. Wozniak, *Phys. Rev. C*, 2003, **68**, 64 601.
15 J. Xu and G. Stell, *J. Chem. Phys.*, 1988, **89**, 1101.
16 E. Vakarin, Y. Duda and M. Holovko, *J. Stat. Phys.*, 1997, **88**, 1333.
17 A. Geiger, F. H. Stillinger and A. Rahman, *J. Chem. Phys.*, 1979, **70**, 4185.
18 R. L. Blumberg, E. H. Stanley, A. Geiger and P. Mausbach, *J. Chem. Phys.*, 1984, **80**, 5230.
19 A. Oleinikova, I. Brovchenko, A. Geiger and B. Guillot, *J. Chem. Phys.*, 2002, **117**, 3296.
20 I. Brovchenko and B. Guillot, *Fluid Phase Eq.*, 2001, **183–184**, 311.
21 W. L. Jorgensen, J. Chandrasekhar and J. D. Madura, *J. Chem. Phys.*, 1983, **79**, 926.
22 J. Chandrasekhar and W. L. Jorgensen, *J. Chem. Phys.*, 1982, **77**, 5073.
23 J. Lejcek, J. P. Matous, J. P. Novak and J. Pick, *J. Chem. Therm.*, 1975, **7**, 927.
24 A. Z. Panagiotopoulos, N. Quirke, M. Stapleton and D. J. Tildesley, *Mol. Phys.*, 1988, **63**, 527.
25 H. Furukawa and K. Binder, *Phys. Rev. A*, 1982, **26**, 556.
26 K. Binder, *Physica A*, 2003, **319**, 99.
27 P. Virnau, L. G. MacDowell, M. Muller and K. Binder, to appear in *Comput. Simul. Stud. Condens. Matter Phys. XVI*, *Springer Proc. Phys.*, 2004.
28 M. Pleimling and A. Huller, *J. Stat. Phys.*, 2001, **104**, 971.
29 M. E. Fisher, *private communication*.
30 Y. Guissani and B. Guillot, *J. Chem. Phys.*, 1993, **98**, 8221.
31 M. Misawa, *J. Chem. Phys.*, 2002, **116**, 8463.
32 I. Brovchenko, D. Paschek and A. Geiger, *J. Chem. Phys.*, 2000, **113**, 5026.
33 G. Gareri, A. Giansanti and J. A. Rupley, *Phys. Rev. A*, 1988, **37**, 2703.
34 A. Bonincontro, G. Careri, A. Giansanti and F. Pedone, *Phys. Rev. A*, 1988, **38**, 6446.
35 F. Bruni, G. Careri and J. S. Clegg, *Biophys. J.*, 1989, **55**, 331.
36 R. Kimmich, F. Klammler, V. D. Skirda, I. A. Serebrennikova, A. I. Maklakov and N. Fatkullin, *Appl. Magn. Res.*, 1993, **4**, 425.
37 A. A. Konsta, J. Laudat and P. Pissis, *Soid State Ionics*, 1997, **97**, 97.
38 P. Pissis and A. A. Konsta, *J. Phys. D*, 1999, **23**, 932.
39 J. Fitter, R. E. Lechner and N. A. Dencher, *J. Phys. Chem.*, 1999, **103**, 8036.